

## Original Article

# Positive allosteric regulation of PAC1-R up-regulates PAC1-R and its specific ligand PACAP

 Guangchun Fan<sup>1,†</sup>, Zhengxin Tao<sup>1,†</sup>, Shang Chen<sup>1</sup>, Huahua Zhang<sup>5</sup>, and Rongjie Yu<sup>1,2,3,4,\*</sup>

<sup>1</sup>Department of Cell Biology, College of Life Science and Technology, Jinan University, Guangzhou 510630, China, <sup>2</sup>Guangdong Province Key Laboratory of Bioengineering Medicine, Guangzhou 510630, China, <sup>3</sup>Guangdong Provincial Biotechnology Drug & Engineering Technology Research Center, Guangzhou 510630, China, <sup>4</sup>National Engineering Research Center of Genetic Medicine, Guangzhou 510630, China, and <sup>5</sup>Department of Medical Genetics, Guangdong Medical University, Dongguan 523000, China

<sup>†</sup>These authors contributed equally to this work.

\*Correspondence address. Tel: +86-13392625921; E-mail: [rongjie\\_yu1123@163.com](mailto:rongjie_yu1123@163.com) / [tyrj@jnu.edu.cn](mailto:tyrj@jnu.edu.cn)

Received 7 December 2021 Accepted 9 February 2022

## Abstract

PAC1-R is a recognized preferential receptor for the neuropeptide of pituitary adenylate cyclase-activating polypeptide (PACAP), which mediates neuroprotective and nerve regenerative activities of PACAP. In this study, we found that in both PAC1R-CHO cells with high expression of PAC1R-eGFP and retinal ganglion cells (RGC-5) with the natural expression of PAC1-R, oligo-peptide PACAP(28-38) and the positively charged arginine-rich penetrating peptide TAT, as positive allosteric modulators of PAC1-R, significantly trigger the nuclear translocation of PAC1-R. The chromatin immunoprecipitation (ChIP)-PCR results show that the nuclear translocated PAC1-R binds with the promoter regions of *PAC1-R* and its specific ligand *PACAP*. The up-regulated promoter activities of *PAC1-R* and *PACAP* induced by PACAP(28-38) or TAT are positively correlative with the increase of the expression levels of PAC1-R and PACAP. Moreover, the nuclear translocation of PAC1-R induced by PACAP(28-38) or TAT is significantly inhibited by the mutation of PAC1-R on Cys25 and the palmitoylation inhibitor 2-bromopalmitate. Meanwhile, the increase in both PAC1-R and PACAP levels and the neuroprotective activities of PACAP(28-38) and TAT in MPP-induced cell model of Parkinson's disease are synchronously inhibited by 2-bromopalmitate, which are positively correlated with the nuclear translocation of PAC1-R induced by PACAP(28-38) or TAT. Bioinformatics analysis and motif enrichment analysis following ChIP-sequencing show that the transcription factors including SP1, Zic2, GATA1, REST and YY1 may be recruited by nuclear PAC1-R and involved in regulating the promoter activities of *PAC1-R* and *PACAP*. ChIP-sequencing and related bioinformatics analysis show that the downstream target genes regulated by the nuclear PAC1-R are mostly involved in the process of cellular stress and related to neuroprotection, neuronal genesis and development.

**Key words** PACAP, PAC1-R, positive allosteric modulation, nuclear translocation

## Introduction

Pituitary adenylate cyclase-activating polypeptide (PACAP) is a neuropeptide with high expression in the central nervous system and peripheral nervous system, belonging to the secretin/growth hormone-releasing hormone/vasoactive intestinal peptide family [1]. PAC1-R is a recognized preferential receptor of PACAP [2], which mediates most activities of PACAP as conservative neurotransmitter and neuromodulator with the effects of neuroprotection [3], neurodevelopment [4] and nerve regeneration [5]. PACAP has two forms including PACAP38 and its N-terminal truncated form

PACAP27 [6], with PACAP38 showing significantly more complete and effective activity than PACAP27 on the activation of PAC1-R [2].

PAC1-R mediates significant anti-inflammatory effect [7] and anti-apoptotic response [8], and promotes neurogenesis [9]. It has been reported that PAC1-R mediates the significant therapeutic effect of PACAP against Alzheimer's disease, Parkinson's disease (PD), Huntington's disease, traumatic brain injury, and stroke in *in vivo* and *in vitro* models [10]. Therefore, PAC1-R serves as an important target for neurological disease drug development [11,12]. PAC1-R belongs to the class B G-protein-coupled receptor (GPCR)

and has a significantly larger N-terminal extracellular domain (PAC1-EC1) than other GPCR members [13], indicating that PAC1-EC1 may recognize not only its authentic ligands but also the allosteric modulators. As for PAC1-R's specific ligand, the different motifs of PACAP play different regulatory roles in the activation of PAC1-R; among them, PACAP(1-5) is responsible for activating PAC1-R [14], while PACAP(6-38) is a full antagonist of PAC1-R [15]. Our previous study showed that PACAP(28-38) (GKRYKQRVKNK) binds to the allosteric regulatory site through both conformational and charge interaction [16,17]; meanwhile the positively charged arginine-rich penetrating peptide TAT (GRKKRRQRRRP) with similar helix structure and amphipathicity to PACAP(28-38) [18] also binds to the same allosteric regulatory site mainly through charge interaction [19]. Furthermore, it has been reported that PACAP(28-38) and TAT not only bind to the same positive allosteric regulatory site in PAC1-EC1 [18], but also display significant cytoprotective activities [20,21]. Based on these findings, we hypothesized that the positive allosteric modulation site of PAC1-R recognized by PACAP(28-38) and TAT may be novel drug targets in PAC1-R for neuroprotection.

Our previous research showed that PACAP38, but not PACAP27, and cellular oxidative stress induce the nuclear translocation of PAC1-R and up-regulate PAC1-R's own expression in a positively correlated way with the nuclear translocation of PAC1-R [22,23]. Therefore, In this study, we tried to clarify the relationship between nuclear translocation of PAC1-R induced by PACAP(28-38) or TAT and their cytoprotective activities in 1-methyl-4-phenylpyridinium (MPP)-induced Parkinson's disease (PD) cell model and explored the role and function of the nuclear-translocated PAC1-R. Our preliminary results showed for the first time that PACAP(28-38) and TAT also significantly induced the nuclear translocation of PAC1-R in PAC1R-CHO cells with high expression of PAC1-R and mouse retinal ganglion cells (RGC-5) with the natural expression of PAC1-R. Our findings suggest that the nuclear translocated PAC1-R is involved in the expression of itself and its specific ligand PACAP, which contributes to the neuroprotective activity of PACAP(28-38) and TAT.

## Materials and Methods

### Materials and cell lines

The Chinese hamster ovary cell line (CHO-K1) and mouse retinal ganglion cell line (RGC-5) were provided by the Shanghai Institutes for Biological Sciences (Shanghai, China). Oligo-peptides PACAP(28-38) and TAT with 95% purity were synthesized by GL Biochem (Shanghai, China). The purity of the peptide was confirmed by reversed-phase high performance liquid chromatography (HPLC) and characterized by matrix-assisted laser desorption/ionization time of flight (MALDI-TOF) mass spectrometry.

### Cell culture and transfection

CHO-K1 cells were grown in Dulbecco's modified Eagle's medium (DMEM; Gibco, Carlsbad, USA) supplemented with 10% fetal calf serum (FBS; Gibco) in humidified atmosphere of 95% air and 5% CO<sub>2</sub> at 37°C. The CHO-K1 cells at logarithmic phase were digested and seeded into 6-well plates at a density of  $2 \times 10^5$  cells/mL. The cells were transfected with vector constructs expressing wild-type PAC1-R tagged with eGFP at the C-terminus (PAC1R-eGFP) or its mutant of Cys25/Ala25 (M-PAC1R-eGFP) [24] using lipofectamine LTX and Opti-MEM medium (Invitrogen, Carlsbad, USA) following

the manufacturer's instructions. For stable expression, cells transfected with plasmids were selected based on G418 (0.8–1 mg/mL) insensitivity, cloned by successive cycles of limiting dilution and screened by detecting the eGFP fluorescence signal. At least three cell clones expressing PAC1R-eGFP or M-PAC1R-eGFP at similar receptor levels were used in parallel in the subsequent experiments. The RGC-5 cells were seeded into 6-well plates at  $2 \times 10^5$  cells/well and cultured in F12 medium (Gibco) containing 10% FBS at 37°C with 5% CO<sub>2</sub> to 80% confluence.

### Molecular docking

The optimized PAC1-R 3D structure acquired from homology modeling was selected as the initial conformation for the docking study utilizing the Discovery Studio 2.5 (DS2.5) software. The binding sites were defined according to the PAC1-R N-terminal EC domain and PACAP(6–38) structure complex (PDB ID: 2JOD). The pre-processing of the PAC1-R 3D structure was implemented using Accelrys DS2.5. The 3D structure of TAT was sketched in DS2.5 and stored as structure data file following energy minimization. The docking procedure was implemented using the LibDock program of the DS2.5 simulation software package. PyMol 1.5 (Schrodinger LLC, Portland, USA) was used for visual inspection of the results and graphical representations.

### Isothermal titration calorimetry (ITC) assay

ITC experiment was carried out using a MicroCal iTC200 instrument (MicroCal, Massachusetts, USA). The recombinant PAC1-EC1 protein was prepared following the method reported previously [25]. Both the recombinant PAC1-EC1 protein and peptides were dissolved in Tris buffer (20 mM Tris-HCl, 100 mM NaCl) containing 5% DMSO. A total of 100  $\mu$ L oligopeptide solutions at the concentration of 200  $\mu$ M were titrated into 280  $\mu$ L of 30  $\mu$ M PAC1-EC1. Titrations were performed at  $25.0 \pm 0.2^\circ\text{C}$ . The power reference was set at  $5 \mu\text{cal} \cdot \text{s}^{-1}$  and the stirring rate was 750 rpm to ensure rapid mixing. The volume was 2  $\mu$ L per injection and the interval between injections was 100 s to warrant equilibrium in each titration point. Each titration was composed of 18 independent titrant additions. Background titrations were performed with chemicals in Tris buffer without PAC1-EC1 protein and with PAC1-EC1 protein in Tris buffer without any chemicals. The binding isotherm was obtained by plotting the reaction heat versus the molar ratio of each peptide to PAC1-EC1 protein. Origin 7.0 software from MicroCal was used for data analysis to get the binding indexes associated with the interaction events such as association constant ( $K_a$ ) and entropy value ( $\Delta H$ ).

### Fluorescence confocal microscopy

Cellular trafficking of PAC1R-eGFP and M-PAC1R-eGFP was evaluated after the cells were treated with or without 1  $\mu$ M PACAP(28-38) or 1  $\mu$ M TAT for 15 min by visualizing the fluorescence of eGFP using appropriate spectral settings (excitation at 488 nm and emission at 545 nm) of the confocal microscope (LSM 510 META; Zeiss, Thornwood, USA) equipped with a Plan-Apochromat636/1.4 numerical aperture oil objective. The fluorescence confocal images were captured and subject to analysis using ImageJ 3.0 software. The nuclear translocation efficiency of PAC1-R = fluorescence intensity in the nuclear/fluorescence intensity of the whole cell. The experiments were performed in parallel with at least three replicates and were repeated three times.

### Immunofluorescence analysis

Cellular trafficking of PAC1-R in RGC-5 cells was evaluated by immunofluorescence confocal imaging. The experimental groups were treated with 1  $\mu\text{M}$  PACAP(28-38) or 1  $\mu\text{M}$  TAT with or without 50  $\mu\text{M}$  palmitoylation inhibitor 2-bromopalmitate (BD34319; Bidepharm, Shanghai, China) for 15 min. Then cells were washed twice with PBS, fixed with 4% paraformaldehyde, and permeabilized with 0.2% Triton X-100 for 5 min at room temperature. Afterwards, cells were incubated with rabbit polyclonal antibody against aa 506–525 (LSKSSSQIRMSGLPADNLAT) of human PAC1-R/ADCYAP1R1 which also corresponds to aa 428–447 of mouse PAC1-R isoform (normal/hop) splicing variant used in this study (ab28670; Abcam, Cambridge, UK) for 1 h at room temperature. After being washed twice with PBS, cells were incubated for 1 h with Alexa Fluor® 647-conjugated anti-rabbit antiserum (ab150075; Abcam). Images were taken using a confocal microscope with an excitation wavelength of 647 nm and emission wavelength of 674 nm. Images were analyzed using ImageJ 3.0 to determine the location and the density of fluorescence of PAC1-R. The nuclear translocation efficiency of PAC1-R = fluorescence intensity in the nuclear/fluorescence intensity of the whole cell, and the data were plotted as the folds of the nuclear translocation efficiency of PAC1-R in cells without any treatment. As for the assessment of the expression level of PAC1-R, on the basis of the consistent and standard operation process, the PAC1-R expression level of each cell was presented by the fluorescence intensity of each cell, and the PAC1-R expression level of each treatment was presented by the average fluorescence intensity from ten cells of each treatment. The experiments were performed in parallel with at least three replicates and were repeated three times.

### ChIP-PCR

ChIP was performed using SimpleChIP® Plus Enzymatic Chromatin IP Kit (Cell Signaling Technology, Danvers, USA) according to the manufacturer's instructions. After incubation with 1  $\mu\text{M}$  PACAP(28-38) or TAT for 15 min, RGC-5 cells were collected by centrifugation and incubated with 1% formaldehyde for 10 min at room temperature to cross-link the protein and DNA. After addition of glycine at a final concentration of 125 mM and incubation for 5 min to stop cross-linking, cells were washed twice with pre-chilled PBS by centrifugation at 2000  $g$  for 5 min at 4°C. Cells were lysed and incubated with rabbit polyclonal antibody against aa 506–525 (LSKSSSQIRMSGLPADNLAT) of human PAC1-R/ADCYAP1R1 (ab28670; Abcam) or the negative control of anti-VPAC2 (ab28624, Abcam) which corresponds to aa 419–438 (LQFHRGSRAQSFLQ TETSVI) of Human VIP receptor 2, followed by incubation with the magnetic beads provided with the kit to obtain the DNA complex bound to the antibody. Then the DNA complex was sent to Weston Biological Company (Chongqing, China) for quality inspection. The immune-enriched DNA samples prepared after ChIP were subject to PCR to detect the PAC1-R/PACAP promoter sequence using primers (F: 5'-TGCCAATGTCCCATGTTTCA-3'; R: 5'-TAAGAGTGGTCAG GACCCC-3') targeting the PAC1-R promoter sequence (–2019 bp to –1739 bp) with predicted 280 bp positive product and primers (F: 5'-TAGCAGCATCTTCAGACGCA-3' and R: 5'-GGAGACTTGGT TGCCGAGG-3') targeting the PACAP promoter sequence (–858 bp to –536 bp) with predicted 320-bp positive product. The experiments were performed in parallel with at least three replicates and were repeated three times.

### PAC1-R promoter activity assay

The 2526 bp (–2500 bp to +26 bp) promoter sequence of mouse PAC1-R gene was cloned into the promoter-reporter vector pYr-PromDetect (Yingrun Biological Company, Changsha, China) to construct the recombinant vector pYr-PromDetect-PAC1p as previously described [23]. The PAC1-R promoter locates upstream of the reporter gene encoding renilla luciferase, and the firefly luciferase gene under the HSV-TK promoter was used as an internal reference.

The recombinant vector pYr-PromDetect-PAC1p (500 ng) or blank vector pYr-PromDetect (500 ng) was transfected into RGC-5 cells using Lipofectamine LTX & PLUS Reagent (Invitrogen) according to the manufacturer's protocol. After transfection, cells were incubated in F12 medium containing 10% FBS for 48 h, then the culture medium was removed and serum-free F12 medium was added. The experimental group cells were incubated with increasing concentrations of PACAP(28-38) or TAT (0.01–100  $\mu\text{M}$ ) with or without 50  $\mu\text{M}$  2-bromopalmitate for 15 min. The control group cells were cultured in serum-free basal medium and washed twice with PBS after incubation. Then the cells were treated with reagents provided with the Dual-Luciferase® Reporter Assay System (Promega, Madison, USA) following the manufacturer's instructions. The activities of two luciferases were detected using the Victor3142 multi-label counter (PerkinElmer, Boston, USA). The promoter activity was expressed as the ratio of renilla luciferase activity (promoter-reporter gene) versus firefly luciferase activity (reference gene), and presented as the folds of the data from the cells transfected with the blank vector pYr-PromDetect. The experiments were performed in parallel with at least three replicates and were repeated three times.

### Western blot analysis

RGC-5 cells were treated with increasing concentrations of PACAP (28-38) or TAT (0.01–100  $\mu\text{M}$ ) with or without 2-bromopalmitate (50  $\mu\text{M}$ ) for 30 min. The control group cells were treated with serum-free basal medium only. Total protein was extracted from cells using RIPA buffer containing 50 mM Tris-HCl, pH 7.4, 150 mM NaCl, 20 mM EDTA, 1% Triton X-100, 1% sodium deoxycholate, 1% SDS and protease inhibitors (Beyotime, Shanghai, China) and subject to SDS-PAGE electrophoresis and transfer to PVDF membranes. Membranes were incubated with rabbit polyclonal antibody against aa 506–525 of human PAC1-R/ADCYAP1R1 (ab28670; Abcam) and anti- $\beta$ -actin antibody (ab227387; Abcam), followed by incubation with HRP-conjugated secondary antibody (Thermo Fisher Scientific, Waltham, USA). Protein bands were visualized using an enhanced chemiluminescence (ECL) kit (Beyotime).

### PACAP promoter activity assay

According to sequence from –2500 bp to +26 bp of the transcription initiation site of mouse PACAP gene, the 2526-bp promoter sequence of PACAP was synthesized and cloned into pUC57-simple plasmid for sequencing characterization. Then the PACAP promoter sequence was cleaved from pUC57-simple-PACAP by *Bgl*III and *Xba*I, and ligated to the promoter-reporter vector pYr-PromDetect (Yingrun Biological Company, Changsha, China) cut by *Bgl*II, and *Nhe*I to construct the recombinant vector pYr-PromDetect-PACAP. The characterization of pYr-PromDetect-PACAP was conducted by restriction cleavage with *Bam*HI, which produced two bands theoretically.

The recombinant vector pYr-PromDetect-PACAP (500 ng) or blank vector pYr-PromDetect (500 ng) was transfected into RGC-5 cells using Lipofectamine LTX & PLUS Reagent (Invitrogen). After transfection, cells were cultured for 48 h in F12 medium containing 10% FBS, then the culture medium was removed and serum-free F12 medium was added. The experimental group cells were treated with increasing concentrations (0.01–100  $\mu\text{M}$ ) of PACAP(28-38) or TAT with or without 2-bromopalmitate (50  $\mu\text{M}$ ) for 15 min. Serum-free basal medium was used in the control group, and the cells were washed twice with PBS after incubation. Then the cells were treated using the Dual-Luciferase® Reporter Assay System (Promega) according to the manufacturer's instructions, and the activities of two luciferases were assayed with the Victor 3142 multi-label counter (PerkinElmer). The promoter activity was first expressed as the ratio of renilla luciferase activity (promoter-reporter gene) versus firefly luciferase activity (reference gene), and then was plotted as the fold of the promoter activity from the transfection with blank vector pYr-PromDetect. The experiments were performed in parallel with at least three replicates and were repeated three times.

#### PACAP level determined by ELISA

RGC-5 cells were treated with increasing concentrations (0.01–100  $\mu\text{M}$ ) of PACAP(28-38) or TAT with or without 2-bromopalmitate (50  $\mu\text{M}$ ) for 30 min, and serum-free basal medium was used in the control group cells. After treatment, cells were washed twice with PBS. PACAP concentrations in RGC-5 cells were assayed using PACAP ELISA Kit (Lvyuan Bird Biotechnology, Beijing, China). The PACAP level was further normalized by the protein concentration quantified using BCA protein assay kit (Thermo Fisher Scientific). All experiments were performed with at least four parallel replicates and repeated three times.

#### Cell viability assay

RGC-5 cells ( $4 \times 10^4$ ) were seeded into each well of 96-well plates and incubated with or without PACAP(28-38) or TAT at concentrations ranging from 0.1  $\mu\text{M}$  to 100  $\mu\text{M}$  for 2 h before MPP (8 mM) exposure. Cell viability was measured 24 h after MPP (8 mM) exposure. In brief, 40  $\mu\text{L}$  MTT solution (0.5 mg/mL; Sigma-Aldrich, St Louis, USA) was added into each well after the medium was removed. After incubation for 4 h, 100  $\mu\text{L}$  isopropanol was added to dissolve the formazan formed by the viable cells. The number of viable cells was determined based on the OD<sub>570</sub> value of the solution. The viability of MPP-treated cells was calculated as the percentage of the OD<sub>570</sub> value of cells without MPP exposure. All experiments were performed with at least four parallel replicates and repeated three times.

#### Terminal deoxynucleotidyl transferase dUTP nick end labeling (TUNEL) assay

RGC-5 cells were incubated with or without PACAP(28-38) (1  $\mu\text{M}$ ), TAT (1  $\mu\text{M}$ ), PACAP(28-38) (1  $\mu\text{M}$ ) + 2-bromopalmitate (50  $\mu\text{M}$ ), or TAT (1  $\mu\text{M}$ ) + 2-bromopalmitate (50  $\mu\text{M}$ ) for 2 h before MPP (8 mM) exposure. Twenty four hours after MPP exposure, cell apoptosis was measured using a TUNEL cell apoptosis detection kit (KeyGEN Biotech, Nanjing, China) according to the manufacturer's instruction. Finally, cells were observed and photographed under the confocal microscope following the treatment with DAB reagent provided with the TUNEL kit. The average optical density (AOD) of TUNEL staining in the RGC-5 cells was determined by Image J 3.0.

All experiments were performed with at least four parallel replicates and repeated three times.

#### ChIP-sequencing assay

ChIP was performed using SimpleChIP® Plus Enzymatic Chromatin IP Kit (Cell Signaling Technology) according to the manufacturer's instructions. After treatment with PACAP(28-38) (1  $\mu\text{M}$ ) or TAT (1  $\mu\text{M}$ ) for 15 min, RGC-5 cells were collected by centrifugation and incubated with 1% formaldehyde for 10 min at room temperature to cross-link the protein and DNA. The cells were washed twice with pre-chilled PBS by centrifugation at 2000 *g* for 5 min at 4°C after addition of glycine at a final concentration of 125 mM and incubation for 5 min to stop cross-linking. Cells were lysed and incubated with rabbit polyclonal antibody against aa 506–525 (LSKSSSQIRMSGLPADNLAT) of human PAC1-R/ADCYAP1R1 (ab28670; Abcam), followed by incubation with the magnetic beads provided with the kit to obtain the DNA complex bound to the antibody. Then the DNA complex was sent to Weston Biological Company (Chongqing, China) for sequencing.

The statistical analysis of raw reads was performed using the FastQC software (<http://www.bioinformatics.bbsrc.ac.uk/projects/fastqc/>; Babraham Institute, Cambridge, UK) and was filtered to obtain high-quality clean reads. The clean reads were mapped to the chromosomes of the mouse genome after the quality control was qualified to perform subsequent analysis. The computeMatrix of deepTools software (<https://deeptools.readthedocs.io/en/develop/content/tools/computeMatrix.html>; MaxPlanck Institute for Immunobiology and Epigenetics, Freiburg, Germany) was used to count the signals in the upstream and downstream 2 kb region of the Transcription Start Site (TSS). MACS2 software ([https://hbctraining.github.io/Intro-to-ChIPseq/lessons/05\\_peak\\_calling\\_mac2.html](https://hbctraining.github.io/Intro-to-ChIPseq/lessons/05_peak_calling_mac2.html); Harvard Chan Bioinformatics Core, Cambridge, USA) was used to complete peak calling analysis ( $P \leq 0.005$ ), and the number, width, distribution, etc. of peaks were counted to filter out peak-related genes. The TSS of each peak-related gene was detected by ChIPseeker (<https://bioconductor.org/packages/release/bioc/html/ChIPseeker.html>; Bioconductor, Buffalo, USA). According to the distance between peak and TSS site, the peak number was counted and the distance distribution between peak and TSS site of the gene was analyzed. Then ChIPseeker software was used to calculate the peak distribution in each functional area (any gene that overlaps with the peak is counted as a peak gene). Functional enrichment analysis in Kyoto Encyclopedia of Genes and Genomes (KEGG) pathway analysis was performed using KOBAS tool (<http://kobas.cbi.pku.edu.cn/>), and Gene ontology (GO) analysis was conducted using Goseq R package software (<https://bioconductor.org/packages/release/bioc/html/goseq.html>; Bioconductor).

#### Transcription factor prediction and motif enrichment analysis

Several online softwares were used to predict the transcription factors that may be bound to the 2000-bp promoter sequence (–2000 bp to 0 bp) of mouse PAC1-R gene and mouse PACAP gene. PROMO (<http://algggen.lsi.upc.es/>) is a virtual laboratory for the identification of putative binding sites of transcription factors in DNA sequences from a species or groups of species of interest [26]. We used this database to predict the transcription factors that may be bound to the 2000-bp promoter sequence of PACAP and PAC1-R, the error tolerance rate was set to 0%. hTftarget (<http://bioinfo.life>).

[hust.edu.cn/hTFtarget#!//](http://hust.edu.cn/hTFtarget#!//)) can predict candidate binding sites of transcription factors on given sequence(s) [27]. The query sequence was submitted on the page to get the predicted transcription factors. GeneCards (<https://www.genecards.org/>) is a searchable, integrative database that provides comprehensive, user-friendly information on all annotated and predicted genes [28]. The gene name was submitted on the homepage to get TF information. We re-verified through three databases to improve accuracy. The transcription factors predicted by at least two of the above online databases at same time were retained and considered as valid query results.

JASPAR (<http://jaspar.genereg.net/>) contains a curated, non-redundant set of profiles derived from the published collections of experimentally defined transcription factors binding sites for eukaryotes [29]. The target transcription factors were submitted to the homepage to obtain the binding motif sequence of the transcription factors, which was further used as templates for the corresponding transcription factor binding motif detected by ChIP-seq.

The ChIP-seq data was analyzed using the Homer software (<http://homer.ucsd.edu/homer/motif/>; University of California, San Diego, USA) to predict the motifs on the genomic region where the peak is bound by nuclear PAC1-R. The conservation of the sequence at the peak location was regarded as motifs, which can be used to find possible binding sites of transcription factors. The predicted transcription factors involved in the binding with nuclear PAC1-R were obtained by comparing the motifs enriched by Homer software from ChIP-seq data with the transcription factor binding motif templates from JASPAR database.

### Statistical analysis

Statistical analysis was performed with GraphPad Prism 5. All data are presented as the mean  $\pm$  SEM. One-way analysis of variance (ANOVA) was used to evaluate the differences among groups. GO/KEGG terms with corrected  $P < 0.05$  were considered significantly enriched by differentially expressed genes. Differences with  $P < 0.05$  were considered to be statistically significant.

## Results

### Molecular docking of TAT with PAC1-EC1

The conformation with the highest LibDock score was selected as the final binding mode of TAT with PAC1-EC1 domain. As shown in Figure 1A, TAT binds with the same site in PAC1-EC1 domain as PACAP(30-37), thus the binding of TAT will produce a steric hindrance for the binding of PACAP(28-38). TAT is predicted to form hydrogen bond interactions with nine amino acid residues in PAC1-EC1 domain, including Asp24, Cys25, Asp111, Asp116, Glu117, Glu119, Ser120, Glu121, Gln125 and Glu359 (Figure 1B). It deserves to be mentioned that Cys25 is the only signal Cys residue not involved in the formation of the conserved disulfide bonds in PAC1-EC1.

In addition, LigScore1, LigScore2, PLP1, PLP2, PMF and PMF04 were used to predict and compare the binding affinities between PAC1-EC1 and oligopeptide TAT and PACAP(28-38). As shown in Table 1, PACAP(28-38) and TAT have similar scores in the affinity parameters determined by computer molecular docking, and the ITC results also confirmed that the binding affinity of TAT with PAC1-EC1 ( $K_d$ ) is similar to that of PACAP(28-38). Furthermore, our previous study has confirmed that both TAT and P(28-38) bind with PAC1-EC1 at the same positiveallosteric site, and the binding affinity of TAT with PAC1-EC1 ( $K_a = (6.35 \pm 0.84) \times 10^5 \text{ M}^{-1}$ ) is similar to that of PACAP(28-38) with PAC1-EC1 ( $K_a = (5.03 \pm 1.59) \times$

$10^5 \text{ M}^{-1}$ ), but when PAC1-EC1 is pre-saturated with PACAP(28-38), no binding signal is detected from the titration of TAT, indicating that the site recognized by TAT in PAC1-EC1 is overlapped by PACAP(28-38) [19].

### Positive allosteric regulation by PACAP(28-38) and TAT induces nuclear translocation of PAC1-R in PAC1R-CHO and RGC-5 cells

To investigate the effect of the positive allosteric regulation on PAC1-R by PACAP(28-38) and TAT on the nuclear translocation of PAC1-R, we tracked a mouse PAC1R-eGFP in CHO cells (named PAC1R-CHO) by confocal microscopy, and found that the nuclear translocation of PAC1R-eGFP can be significantly detected in cells treated with PACAP(28-38) or TAT (Figure 2A), compared with that in the control cells. In addition, a Cys25/Ala25 (M-PAC1-R) mutant, with a mutation in the palmitoylation site (Cys25) which contributes to the formation of the allosteric modulation domain rich in anionic aa residues recognized by cationic Arginine-rich peptide [23], was constructed and expressed in CHO-K1 cells. The results showed that the ability of M-PAC1-R to traffic into the nucleus triggered by PACAP(28-38) or TAT is significantly weaker than that of the wild-type PAC1-R (Figure 2B), indicating that Cys25 and its palmitoylation play key roles not only in the recognition of the positive allosteric modulator such as PACAP(28-38) and TAT, but also in the nuclear translocation of PAC1-R. Our results also showed that PACAP(28-38) and TAT not only induce significant nuclear translocation of PAC1-R but also increase the PAC1-R level in RGC-5 cells. Furthermore, both the nuclear translocation and the up-regulation of PAC1-R induced by PACAP(28-38) or TAT are effectively inhibited by palmitoylation inhibitor 2-bromopalmitate (Figure 2C,D).

### Positive allosteric regulation by PACAP(28-38) and TAT enhances the promoter activity and expression level of PAC1-R

In order to explore the relationship between the nuclear translocation of PAC1-R and the expression up-regulation of PAC1-R induced by PACAP(28-38) or TAT, ChIP was performed using the antibody targeting the C-terminus of PAC1-R and the nuclear extracts from RGC-5 cells treated with 1  $\mu\text{M}$  PACAP(28-38) or TAT. The subsequent ChIP-PCR results showed that the positive band corresponding to the *PAC1-R* promoter-related sequence was amplified with primers F: 5'-TGCCAATGTCCCATGTTTCA-3' and R: 5'-TAA GAGTGGTCAGGACCCCC-3' targeting the PAC1-R promoter sequence (-2019 bp to -1739 bp) (Figure 3A). This positive ChIP-PCR result indicated that the nuclear PAC1-R binds with the *PAC1-R* promoter-related sequence in some way and is involved in the regulation of the promoter activity of *PAC1-R*.

Moreover, the *PAC1-R* promoter reporter vector pYr-PromDetect-PAC1p containing the 2526 bp (-2500 bp to +26 bp) promoter sequence of mouse *PAC1-R* gene was used to detect the effects of PACAP(28-38) and TAT on the *PAC1-R* promoter activity. As shown in Figure 3B, the promoter activity of *PAC1-R* was significantly enhanced by PACAP(28-38) (0.1  $\mu\text{M}$ -1  $\mu\text{M}$ ) or TAT (0.1  $\mu\text{M}$ -1  $\mu\text{M}$ ) in RGC-5 cells. Western blot analysis results also confirmed that the PAC1-R expression was increased positively with the concentrations of PACAP(28-38) and TAT in RGC-5 cells (Figure 3C). Meanwhile, the PAC1-R truncated form (about 35 kDa), which represents the truncated forms of PAC1-R in the nuclear fraction [23], was

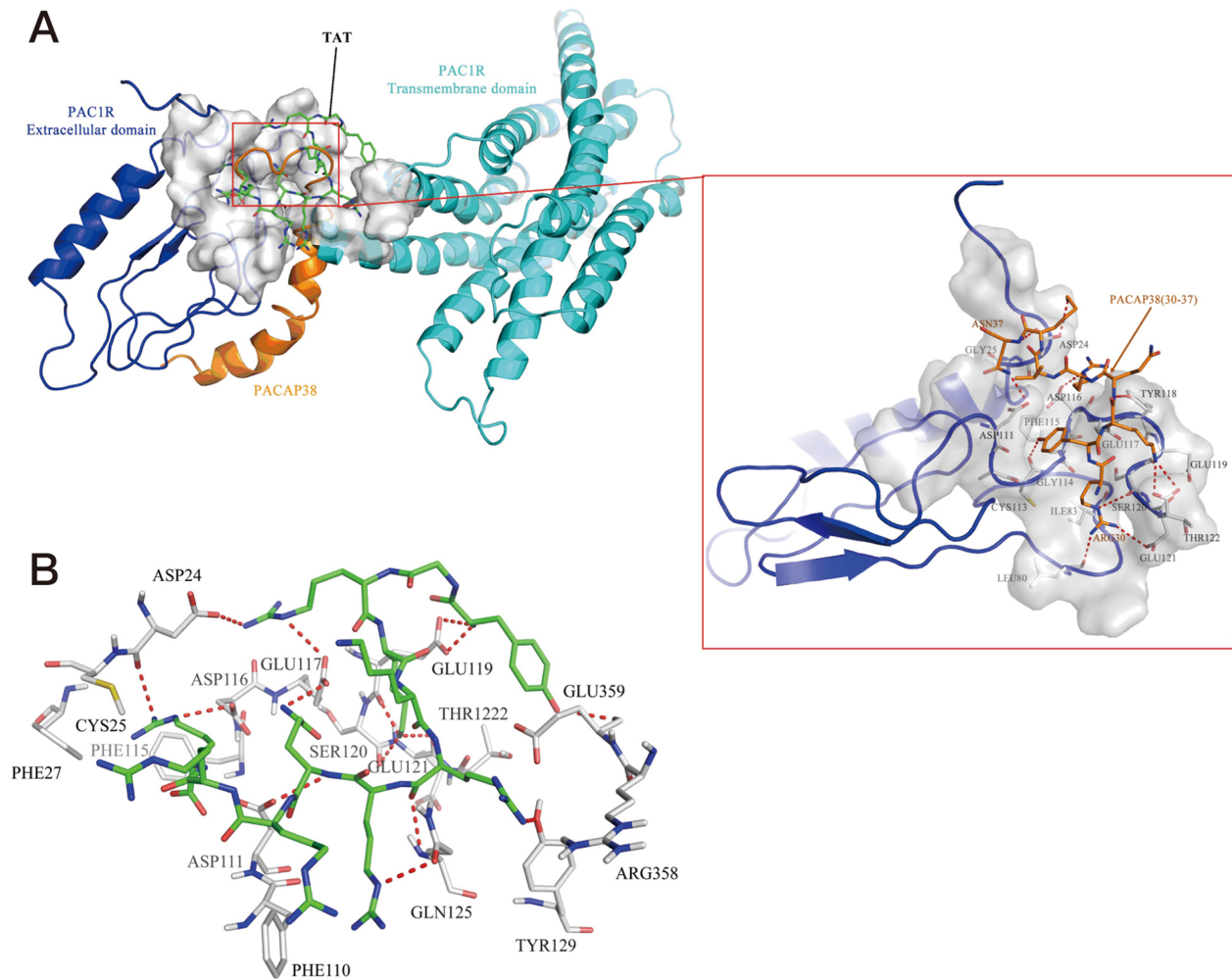


**Figure 1. Molecular docking of TAT on PAC1-R** (A) The predicted binding sites of TAT on PAC1-R, with PACAP38 superimposed according to the resolved complex 3D structure of PACAP38 with the extracellular domain of PAC1-R (PDB code: 2JOD). PAC1-R in deep blue and PACAP38 in yellow are shown as cartoon style and the binding small molecules are shown as sticks. The binding site is represented by the surface model. The red frame indicates the details of the binding mode of PACAP38(30-37) with PAC1-R showing that TAT and P(28-38) share the most common interacting residues. (B) The details of the predicted binding mode of TAT with PAC1-R. The contact residues are shown and labeled by type and number. The red dotted line illustrates the hydrogen bond interaction.

**Table 1. The binding affinities of antibiotics or oligopeptides with PAC1-EC1 calculated by molecular docking and ITC**

Scoring	LigScore1	LigScore2	PLP1	PLP2	PMF	PMF04	$K_a$ from ITC ( $M^{-1}$ )
P(28-38)	10.24	10.21	134.26	109.6	182.02	142.5	$(6.35 \pm 0.84) \times 10^5$
TAT	9.78	9.65	96.75	107.43	153.87	125.6	$(5.03 \pm 1.59) \times 10^5$

induced by PACAP(28-38) or TAT, also indicating that the positive allosteric modulator PACAP(28-38) and TAT induce significant nuclear translocation of PAC1-R (Figure 3C).

All the above data showed that the nuclear translocation of PAC1-R induced by PACAP(28-38) and TAT contributes to the up-regulation of the promoter activity and expression of PAC1-R itself, and the translocated PAC1-R binds with the promoter sequence of *PAC1-R* in some way.

#### Positive allosteric regulation by PACAP(28-38) and TAT enhances the promoter activity and expression level of PACAP

The ChIP was performed using the antibody targeting the C-termi-

nus of PAC1-R and the nuclear extracts from RGC-5 cells treated with  $1 \mu M$  PACAP(28-38) or TAT to further investigate the role of allosteric regulation of PAC1-R in the relationship between nuclear translocation of PAC1-R and PACAP expression. The subsequent ChIP-PCR result showed that the positive band corresponding to the *PACAP* promoter-related sequence was amplified with primers F: 5'-TAGCAGCATCTTCAGACGCA-3' and R: 5'-GGAGACTTGTGGCCGAG-3' targeting the *PACAP* promoter sequence (-858 bp to -536 bp) (Figure 3D), indicating that the nuclear PAC1-R binds with the *PACAP* promoter-related sequence in some way and is also involved in the regulation of the promoter activity of *PACAP*.

Then the *PACAP* promoter reporter vector pYr-PromDetect-PACAP containing the 2526 bp (-2500 bp to +26 bp) promoter

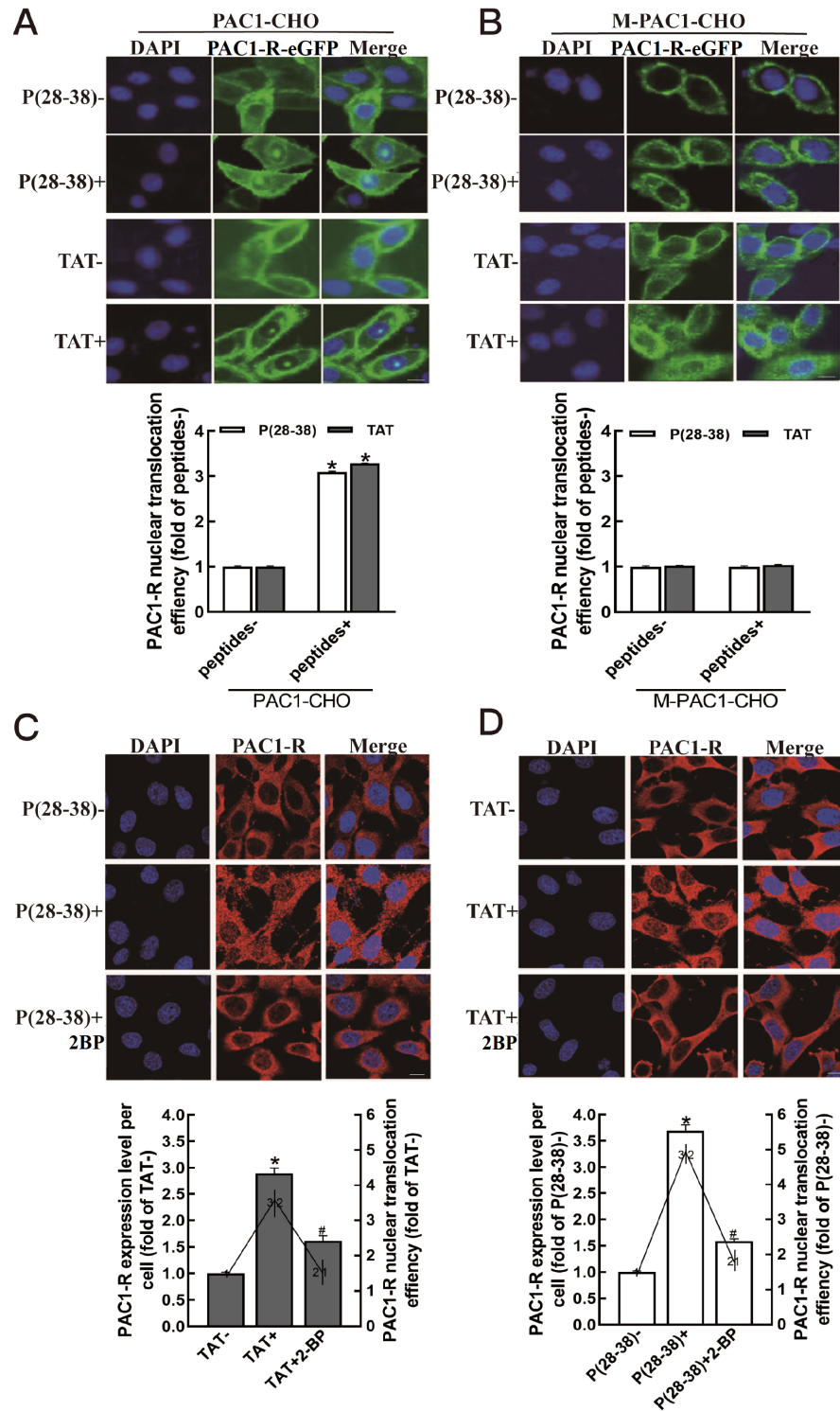


**Figure 2.** Fluorescence confocal microscopy and immunofluorescence analysis on the nuclear translocation of PAC1-R induced by PACAP(28-38) and TAT in PAC1-CHO and RGC-5 cells. PACAP(28-38) and TAT induce nuclear translocation of PAC1-R in PAC1-CHO cells, and PACAP(28-38) and TAT promote PAC1-R expression, which is positively correlated with the nuclear translocation of PAC1-R in RGC-5 cells. (A) Fluorescence microscope imaging (upper) and corresponding statistical analysis (lower) showed that PACAP(28-38) and TAT induce significant trafficking and aggregation of PAC1R-eGFP fluorescence signal (green) into the nucleus of PAC1-CHO cells. \* $P < 0.01$  vs peptides-. (B) PACAP(28-38) and TAT can not induce significant trafficking or aggregation of M-PAC1R(Cys25/Ala25)-eGFP fluorescence signal (green) into the nucleus of M-PAC1-CHO cells. \* $P < 0.01$  vs peptides-. (C,D) The results of immunofluorescence confocal imaging (upper) and the corresponding immunofluorescence signal data analysis (lower) showed that both PACAP(28-38) and TAT can significantly induce the nuclear translocation of PAC1-R and up-regulate the expression level of PAC1-R, and both are significantly inhibited by 2-bromopalmitate. Data are presented as the mean  $\pm$  SEM of three experiments. \* $P < 0.01$  vs TAT- or P(28-38)-. # $P < 0.01$  vs TAT+. Scale bar = 5  $\mu$ m. P(28-38): PACAP(28-38).

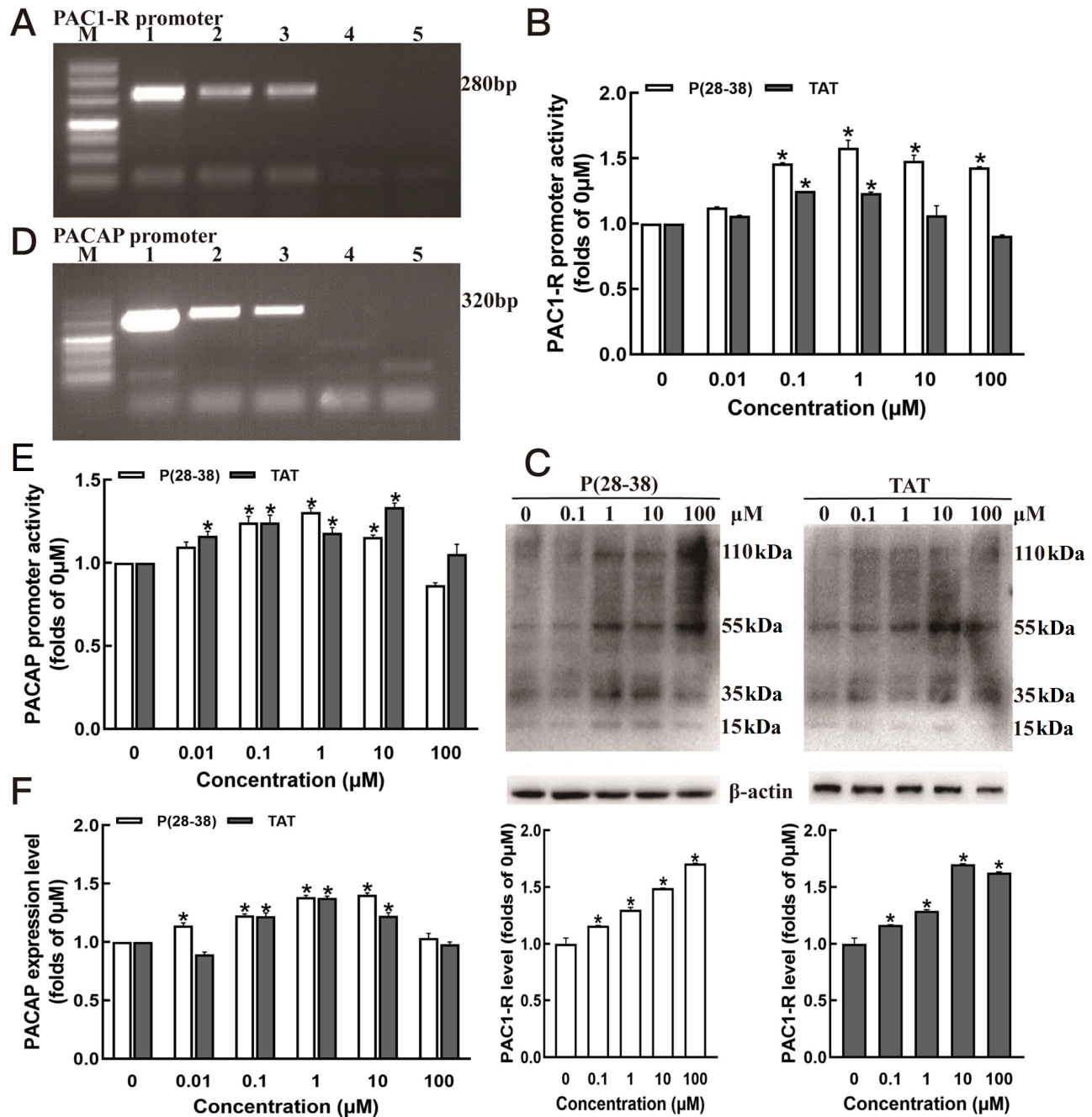


**Figure 3. PACAP(28-38) and TAT increase both the promoter activities and expression levels of PAC1-R and PACAP** (A) The ChIP-PCR results obtained by using nuclear extracts of RGC-5 cells with the primers of F: 5'-TGCCAATGTCCCATGTTTCA-3' and R: 5'-TAAGAGTGGTCAGGACCC-3' targeting PAC1-R promoter sequence (-2019 bp to -1739 bp). The positive 280bp band illustrates the binding of the C-terminus of PAC1-R with the PAC1-R promoter sequence in some way. (B) The dual-luciferases reporter assay results showed that the promoter activity of *PAC1-R* is significantly enhanced by PACAP(28-38) (0.1–100  $\mu\text{M}$ ) and TAT (0.1–1  $\mu\text{M}$ ). (C) Western blots of PAC1-R in whole RGC-5 cells incubated with PACAP(28-38) or TAT in concentrations from 0.1  $\mu\text{M}$  to 100  $\mu\text{M}$  (upper) and the corresponding statistical analysis (lower). (D) The ChIP-PCR results obtained by using nuclear extracts of RGC-5 cells with the primers of F: 5'-TAGCAGCATCTTCAGACGCA-3' and R: 5'-GGAGACTTGTGGCCGAGG-3' targeting PACAP promoter sequence (-858 bp to -536 bp). The positive 320 bp band illustrated the binding of the C-terminus of PAC1-R with the PACAP promoter sequence in some way. (E) The dual-luciferases reporter assay result showed that the promoter activity of PACAP is significantly enhanced by PACAP(28-38) (0.1  $\mu\text{M}$ –10  $\mu\text{M}$ ) and TAT (0.01  $\mu\text{M}$ –10  $\mu\text{M}$ ). \* $P < 0.01$  vs 0  $\mu\text{M}$ . (F) The ELISA result showed that PACAP(28-38) (0.01  $\mu\text{M}$ –10  $\mu\text{M}$ ) and TAT (0.1  $\mu\text{M}$ –10  $\mu\text{M}$ ) significantly increase the expression level of PACAP. Data are presented as the mean  $\pm$  SEM of three experiments. \* $P < 0.01$  vs 0  $\mu\text{M}$ . (A,D) ChIP-PCRs were conducted with templates including: 1, the nuclear extraction of RGC-5 cells before precipitation by the antibody targeting the C-terminus of PAC1-R; 2, ChIP product from RGC-5 cells treated with PACAP(28-38) (1  $\mu\text{M}$ ) with PAC1-R antibody; 3, ChIP product from RGC-5 cells treated with TAT (1  $\mu\text{M}$ ) with PAC1-R antibody; 4, ChIP product from RGC-5 cells treated with PACAP(28-38) (1  $\mu\text{M}$ ) with antibody targeting VPAC2-R; 5, ChIP product from RGC-5 cells treated with TAT (1  $\mu\text{M}$ ) with antibody targeting VPAC2-R; M, DNA marker. P(28-38): PACAP(28-38).



sequence of mouse *PACAP* gene was transfected into RGC-5 cells to investigate the effects of PACAP(28-38) and TAT on the *PACAP* promoter activity. As shown in Figure 3E, the promoter activity of *PACAP* was significantly enhanced by PACAP (28-28) (0.1  $\mu$ M–10  $\mu$ M) or TAT (0.01  $\mu$ M–10  $\mu$ M) in RGC-5 cells, which is consistent with the subsequent ELISA results of PACAP expression level (Figure 3F). These results indicated that at the concentrations of 0.1  $\mu$ M–10  $\mu$ M, both PACAP(28-38) and TAT increased the promoter activity and expression level of PACAP. However, at concentrations over 10  $\mu$ M, the positive effects of PACAP(28-38) and TAT on PACAP's promoter activity and expression level were decreased.

All the above data showed that the nuclear translocation of PAC1-R induced by PACAP(28-38) or TAT contributes to the up-regulation of the promoter activity and expression level of PAC1-R's specific ligand PACAP and the nuclear translocated PAC1-R binds with the promoter sequence of PACAP in some way.

### Palmitoylation inhibitor interferes with the promoter activities and expression levels of PAC1-R and PACAP induced by PACAP(28-38) and TAT

It has been reported that palmitoylation inhibitor 2-bromopalmitate can inhibit oxidative stress-induced nuclear translocation and the corresponding increase of PAC1-R expression [23]. In this study, the palmitoylation inhibitor 2-bromopalmitate was also found to play an inhibitory role in the up-regulation of PAC1-R and PACAP induced by PACAP(28-38) or TAT. The dual-luciferases reporter assays showed that the increases of promoter activities of *PAC1-R* and *PACAP* induced by PACAP(28-38) or TAT were both significantly inhibited by 50  $\mu$ M of 2-bromopalmitate (Figure 4A,B). Western blot analysis and ELISA results also confirmed that the increases of the expression levels of PAC1-R and PACAP induced by PACAP(28-38) or TAT were inhibited by 50  $\mu$ M of 2-bromopalmitate (Figure 4C,D). Furthermore, the decrease of the truncated forms of PAC1-R with molecular weight smaller than 35 kDa also indicated that the nuclear translocation of PAC1-R was inhibited by 50  $\mu$ M of 2-bromopalmitate (Figure 4C). All these results showed that the increased levels of PAC1-R and PACAP are positively correlated with the nuclear translocation of PAC1-R induced by PACAP(28-38) or TAT.

### The neuroprotective activities of PACAP(28-38) and TAT are mediated by PAC1-R

MPP-treated PD cell model was used to examine the neuroprotective activities of PACAP(28-38) and TAT. The MTT assay results showed that treatment with 8 mM MPP caused significant apoptosis in RGC-5 cells, which caused about 31% of cells remain viable (Figure 5A-C). PACAP(28-38) or TAT, at concentrations of 0.1–100  $\mu$ M, significantly blocked the decrease of cell viability induced by MPP (Figure 5A), and the cytoprotective effects of PACAP (28-38) and TAT were significantly inhibited by 100 nM of the PAC1-R antagonist PACAP(6-38) (Figure 5B), which indicated that the cytoprotective effects of PACAP(28-38) and TAT were mediated by PAC1-R. Moreover, palmitoylation inhibitor 2-bromopalmitate significantly inhibited the cytoprotective activities of PACAP(28-38) and TAT (Figure 5C), confirming that the nuclear translocation of PAC1-R plays a key role in the cytoprotective effects of these two oligopeptide.

TUNEL assay results also showed that MPP treatment increased

the number of TUNEL-positive cells, while pre-treatment with 10  $\mu$ M PACAP(28-38) or TAT significantly reduced the TUNEL signal, confirming the cytoprotective activities of PACAP(28-38) and TAT against the apoptosis induced by MPP in RGC-5 cells, and the anti-apoptotic activities of PACAP(28-38) and TAT were significantly inhibited by 50  $\mu$ M 2-bromopalmitate.

All the above results indicated that the nuclear translocation and the subsequent up-regulation of PAC1-R/PACP were positively correlated with the cytoprotective activities of PACAP(28-38) and TAT.

### ChIP-seq analysis of transcription factors bound with nuclear translocated PAC1-R in *PACAP* and *PAC1-R* promoters

Since the ChIP-PCR results indicated that the nuclear translocated PAC1-R binds with the promoters of *PAC1-R* and *PACAP* in some way, we hypothesize that some transcription factors may be involved in the binding of nuclear PAC1-R with the *PAC1-R* and *PACAP* promoters. Analysis using online software and ChIP-seq combined with motif enrichment analysis were performed to identify the related transcription factors which may be recruited by nuclear PAC1-R to regulate the promoter activities of *PAC1-R* and *PACAP*.

The promoter sequencing for transcription factor binding sites using PROMO, hTFtarget and GeneCards showed that the mouse *PACAP* 2000 bp promoter sequence contains binding sites for 19 (16+2+1) transcription factors as screened out by at least two databases analysis softwares, among which GATA1, Zic2 and Sp1 have been reported (Figure 6A, in blue) [30–33], while the mouse *PAC1-R* 2000 bp promoter sequence has binding sites for 11 (8+2+1) transcription factors as predicted by at least two softwares collectively, among which P53 and Zic2 have been reported (Figure 6B, in blue) [30,31]. These results indicated that our online bioinformatics analysis strategy is reliable, which can screen out the reported transcription factors involved in the regulation of *PACAP* and *PAC1-R* promoter activities successfully.

Furthermore, besides Zic2, five common transcription factors including CTCF, REST, POLR2A, YY1 and EZH2 are shared by both *PACAP* and *PAC1-R* (Figure 6A,B, in italic). Since the nuclear PAC1-R up-regulates the promoter activities of both *PACAP* and *PAC1-R*, we hypothesize that these 6 transcription factors shared by both promoters of *PACAP* and *PAC1-R* may be involved in the binding with nuclear PAC1-R with higher possibility than others.

After comparing the enriched motifs from ChIP-seq and subsequent analysis using Homer software with the standard binding motif templates of transcription factors from JASPAR database and from all transcription factors mention above, we found that among all the reported transcription factors involved in the expression of *PAC1-R* and *PACAP*, only the binding motifs of three transcription factors, including SP1, GATA1 and Zic2, from the reported transcription factors were highly enriched and detected by ChIP-seq and related data analysis (Figure 6C–E), and three of the six common transcription factors shared by both *PACAP* and *PAC1-R*, including Zic2, REST and YY1, were detected by ChIP-seq and motif enrichment analysis (Figure 6E–G).

All the transcription factors successfully screened out by both online software screening and the enrichment analysis of the ChIP-seq data, which target the nuclear PAC1-R, were shown in frames of Figure 6A,B. Since Zic2, REST and YY1 are common transcription

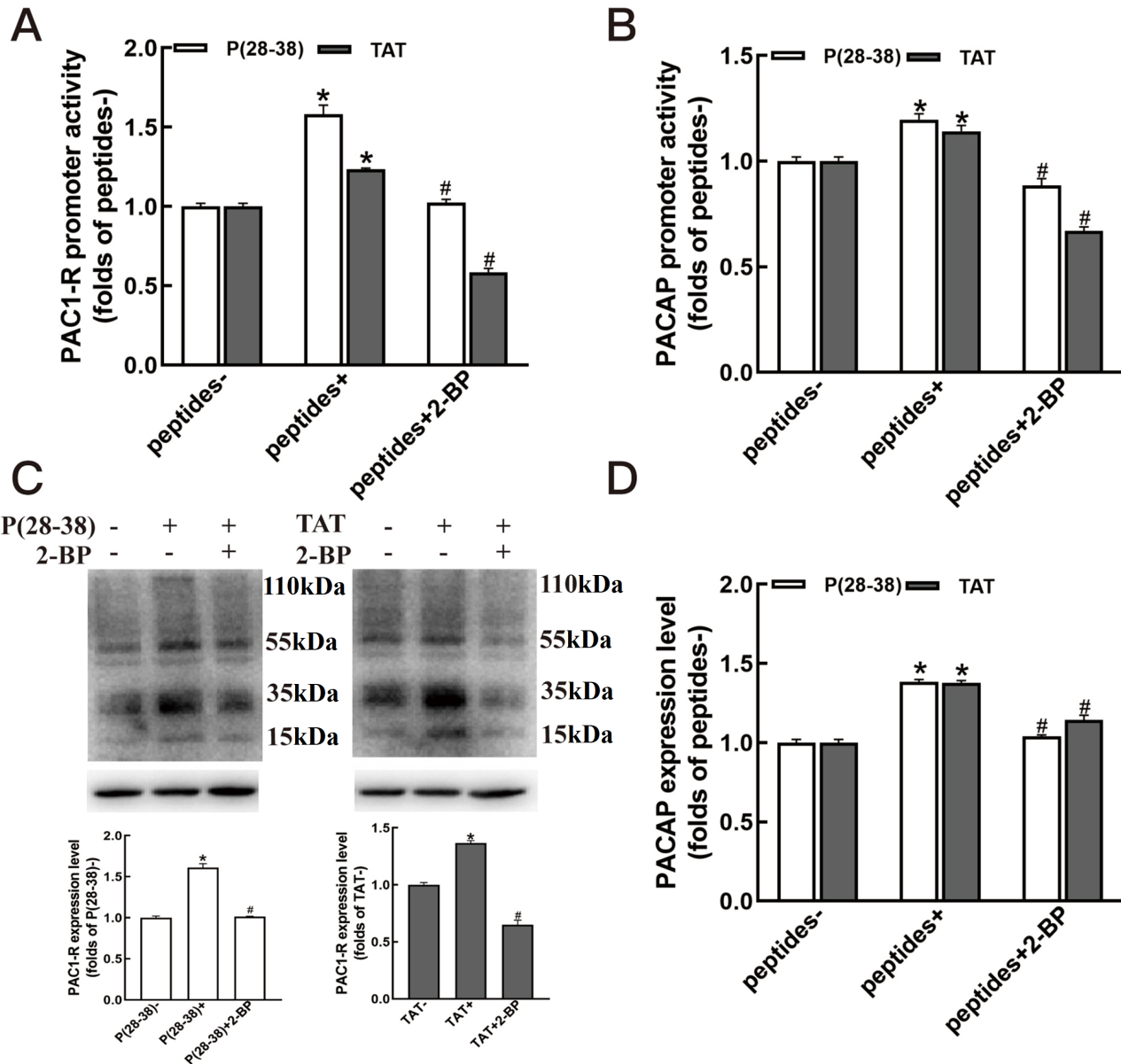


**Figure 4.** Palmitoylation inhibitor 2-bromopalmitate interferes with the promoter activities and expression levels of PAC1-R and PACAP induced by PACAP(28-38) and TAT (A) The dual-luciferases reporter assay result showed that PAC1-R promoter activity induced by PACAP(28-38) and TAT is significantly inhibited by 2-bromopalmitate. (B) The dual-luciferases reporter assay result showed that PACAP promoter activity induced by PACAP(28-38) and TAT is significantly inhibited by 2-bromopalmitate. (C) Western blots (upper) and the subsequent quantitative analysis (lower) showed that the PAC1-R expression level induced by PACAP(28-38) and TAT treatment is significantly inhibited by 2-bromopalmitate. (D) The ELISA result showed that the PACAP expression level induced by PACAP(28-38) and TAT treatment is significantly inhibited by 2-bromopalmitate. Data are presented as the mean  $\pm$  SEM of three experiments. \* $P < 0.01$  vs peptides-, P(28-38)-, or TAT-. # $P < 0.01$  vs peptides+, P(28-38)+, or TAT+. 2-BP: 2-bromopalmitate; P(28-38): PACAP(28-38).

factors shared by both *PACAP* and *PAC1-R* promoters, which are also enriched and detected by ChIP-seq and subsequent data analysis, these three transcription factors have higher possibilities than others to be recruited by nuclear PAC1-R. Further studies are needed to explore their roles in the regulation of the promoter activities of *PAC1-R* and *PACAP* through binding with nuclear PAC1-R.

#### ChIP-seq analysis of direct gene targets regulated by nuclear PAC1-R

Since PAC1-R has been confirmed to undergo nuclear translocation,

the positive result of ChIP-PCR and the successful sequencing of ChIP products using antibody targeting the C-terminus of PAC1-R suggest that the nuclear PAC1-R may be involved in the regulation of other genes. In order to identify the direct downstream gene targets regulated by nuclear PAC1-R and further explore the underlying molecular mechanisms mediated by nuclear-translocated PAC1-R, a genome-wide data analysis following ChIP-seq assay was performed.

Before data processing, 278,144,437 reads per sample (ranging from 24,957,487 to 31,680,115 reads) passed the quality control on

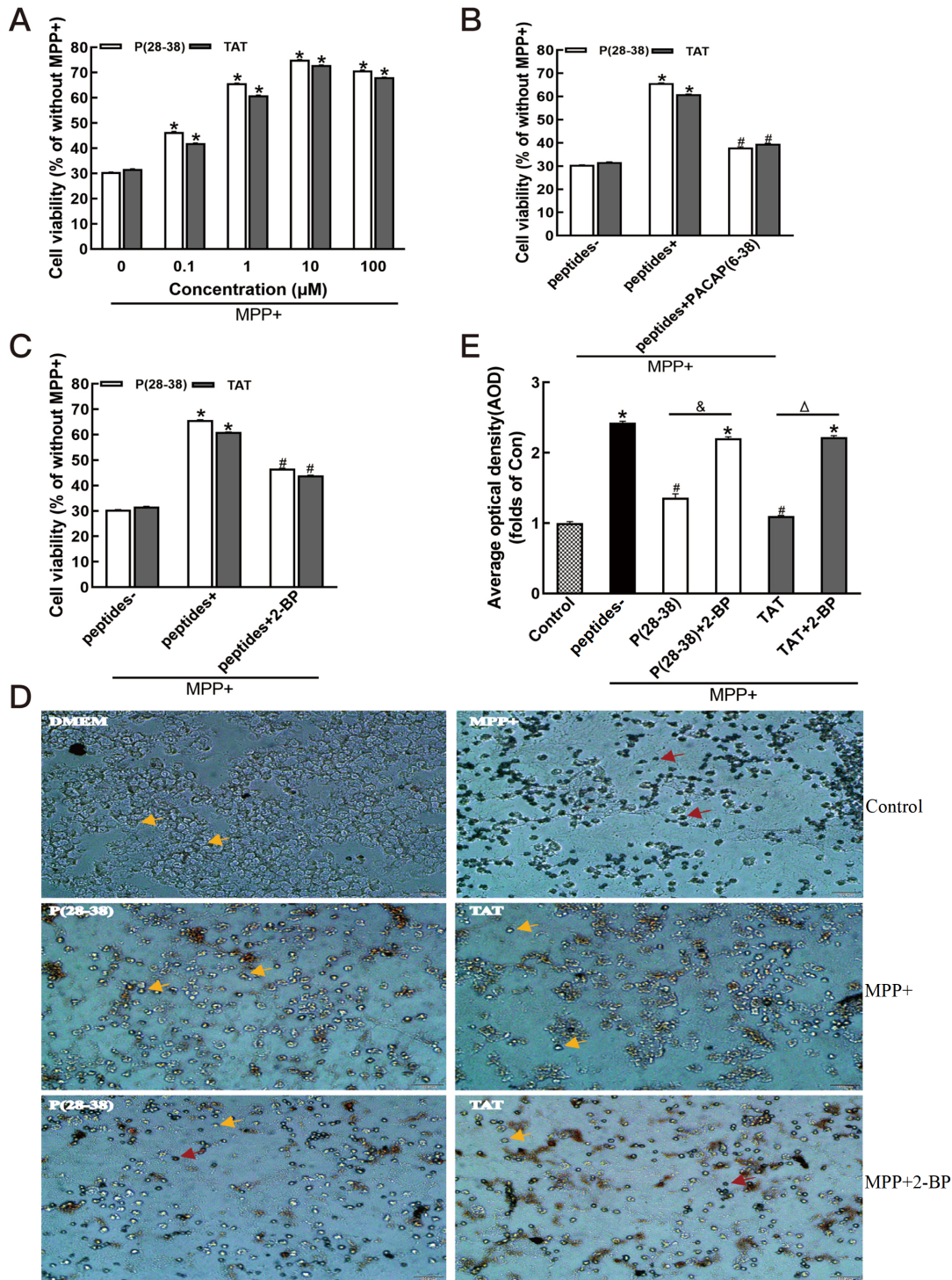


**Figure 5.** Effects of PACAP(28-38) and TAT on the cell viability in RGC-5 cell PD model induced by MPP (A) MTT assay showed that both PACAP(28-38) and TAT in concentrations from 0.1 to 100  $\mu\text{M}$  significantly increase the cell viability decreased by MPP treatment.  $*P < 0.01$  vs 0  $\mu\text{M}$ . (B) MTT assay showed that PACAP(28-38) and TAT have significant cytoprotective effects which are significantly inhibited by PACAP(6-38).  $*P < 0.01$  vs peptides-.  $\#P < 0.01$  vs peptides+. (C) PACAP(28-38) and TAT have significant cytoprotective effects which are significantly inhibited by 2-bromopalmitate.  $*P < 0.01$  vs peptides-.  $\#P < 0.01$  vs peptides+. (D) Effects of PACAP(28-38) and TAT with or without 2-bromopalmitate on apoptosis as determined by TUNEL assay in RGC-5 cells induced by MPP. Microscopic images of cells treated with DMEM without MPP as control (CON) or with 8 mM MPP, PACAP(28-38) + MPP, TAT + MPP, PACAP(28-38) + MPP + 2-BP and TAT + MPP + 2-BP. Yellow arrows indicate non-apoptotic cells and red arrows indicate apoptotic cells (Scale bar = 10  $\mu\text{m}$ ). (E) Quantitative analysis of the TUNEL images showed that PACAP(28-38) and TAT have significant cytoprotective effects which are significantly inhibited by 2-bromopalmitate. Data are presented as the mean  $\pm$  SEM of three experiments.  $*P < 0.01$  vs control.  $\#P < 0.01$  vs peptides-.  $\&P < 0.01$ . 2-BP: 2-bromopalmitate; P(28-38): PACAP(28-38).

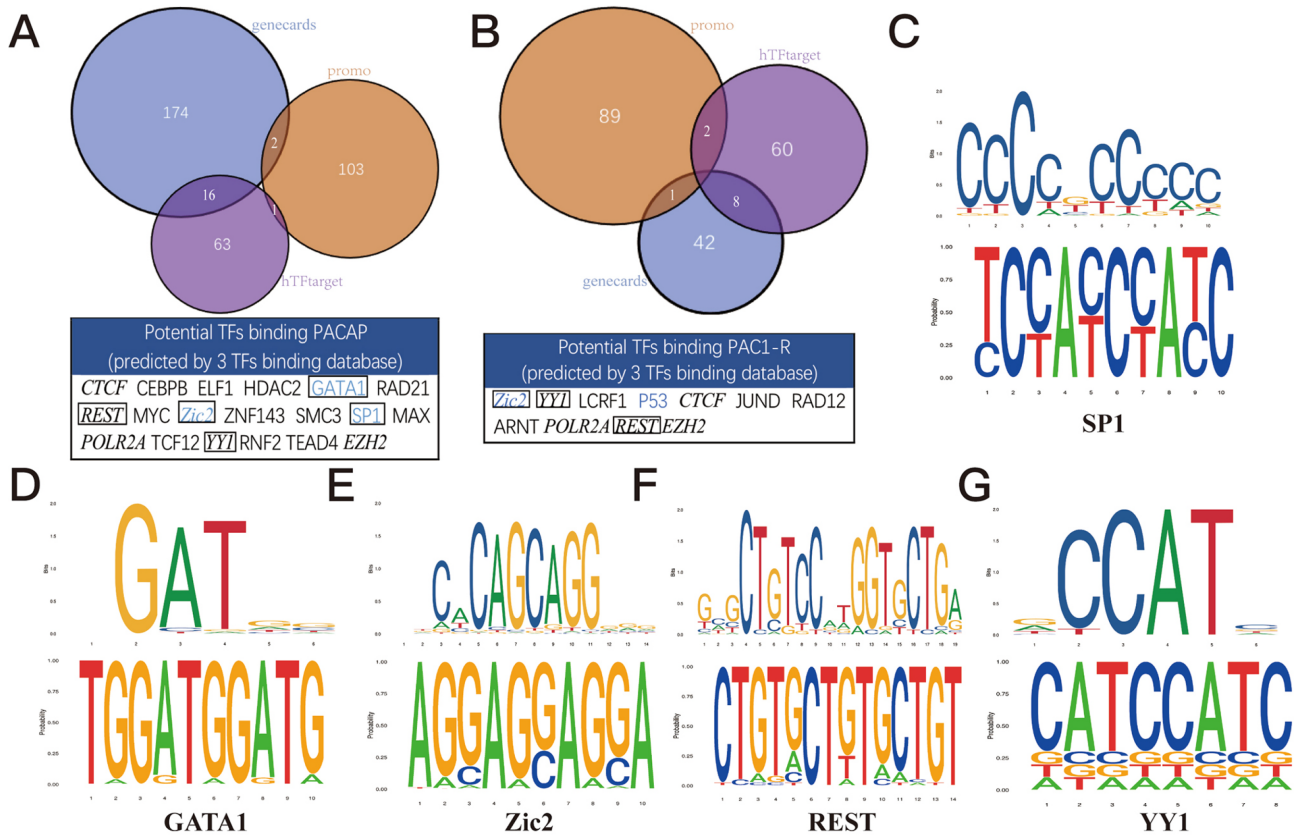


**Figure 6.** ChIP-seq analysis for transcription factors recruited by nuclear-translocated PAC1-R targeting PACAP and PAC1-R promoters (A) The 19 transcription factors of PACAP promoter predicted by at least two databases. (B) The 11 transcription factors of PAC1-R promoter predicted by at least two databases. The blue words indicate the transcription factors reported previously, the italic words indicate the transcription factors shared by promoters of both PACAP and PAC1-R, and the framed words indicate transcription factors highly enriched and detected by ChIP-seq and related data analysis. (C) The comparative analysis of the SP1 standard motif in JASPAR database (upper) with the motif enriched by Homer software following ChIP-seq (lower). (D) The comparative analysis of the GATA1 standard motif in JASPAR database (upper) with the motif enriched by Homer software following ChIP-seq (lower). (E) The comparative analysis of the Zic2 standard motif in JASPAR database (upper) with the motif enriched by Homer software following ChIP-seq (lower). (F) The comparative analysis of the REST standard motif in JASPAR database (upper) with the motif enriched by Homer software following ChIP-seq (lower). (G) The comparative analysis of the YY1 standard motif in JASPAR database (upper) with the motif enriched by Homer software following ChIP-seq (lower). TFs: transcription factors.

average, and 96.8% of total reads were mapped to the *Mus Musculus* genome. Each sample has an average of 20,416 significant peaks (ranging from 18,454 to 22,356). About 20.39% peaks fall into the gene promoter region, and 10.4% distribute in the 1 kb region above and below the promoter (Figure 7A,B). The number of peak genes is about 5797.

KEGG pathway enrichment analysis revealed that several cellular stress, cell protection and neurodegenerative disease pathways, including mTOR signaling pathway, Ubiquitin-mediated proteolysis, p53 signaling pathway, Huntington's disease and Parkinson disease are regulated by nuclear-translocated PAC1-R (Figure 7C).

GO analysis revealed that the downstream target genes regulated by nuclear-translocated PAC1-R participate in diverse biological processes, cell components and molecular functions (Figure 7D). The biological processes include anatomical structure development, regulation of developmental process, and regulation of multicellular organismal process, the cell components include cell projection, and the molecular functions include receptor ligand activity, receptor regulator activity, and enzyme binding.

## Discussion

PACAP(28-38) and TAT are two oligopeptides which have been

confirmed to bind with the same allosteric modulation site in the N-terminal extracellular domain of PAC1-R [18] with similar affinity calculated by molecular docking and ITC assay [19]. In this research, we found for the first time that PACAP(28-38) and TAT induced significant nuclear translocation of PAC1-R in PAC1-R-CHO cells and RGC-5 cells. The nuclear translocation of PAC1-R is inhibited by 2-bromopalmitate, which has been shown to interfere with the palmitoylation of the first and only single CYC25 in PAC1-EC1 [23], leading to both decreased expression levels of PAC1-R/PACAP induced by PACAP(28-38) or TAT and weakened cytoprotective activities of PACAP(28-38)/TAT in a positively-correlated way. Our data indicated that the allosteric modulation site recognized by PACAP(28-38)/TAT of PAC1-R is a potential target for neuroprotective drug development, and that the nuclear translocation of PAC1-R plays a key role in the neuroprotective activity mediated by PAC1-R.

Actually, the nuclear translocation of GPCRs has been detected in epithelial endothelial cells, nerve cells, tumor cells and other cell types, suggesting that GPCRs, either located on the nuclear membrane or entering the nucleus, are closely related to physiological functions such as cytoprotection, damage repair and neurodevelopment [34]. Studies have shown that GPCRs located in the nuclear

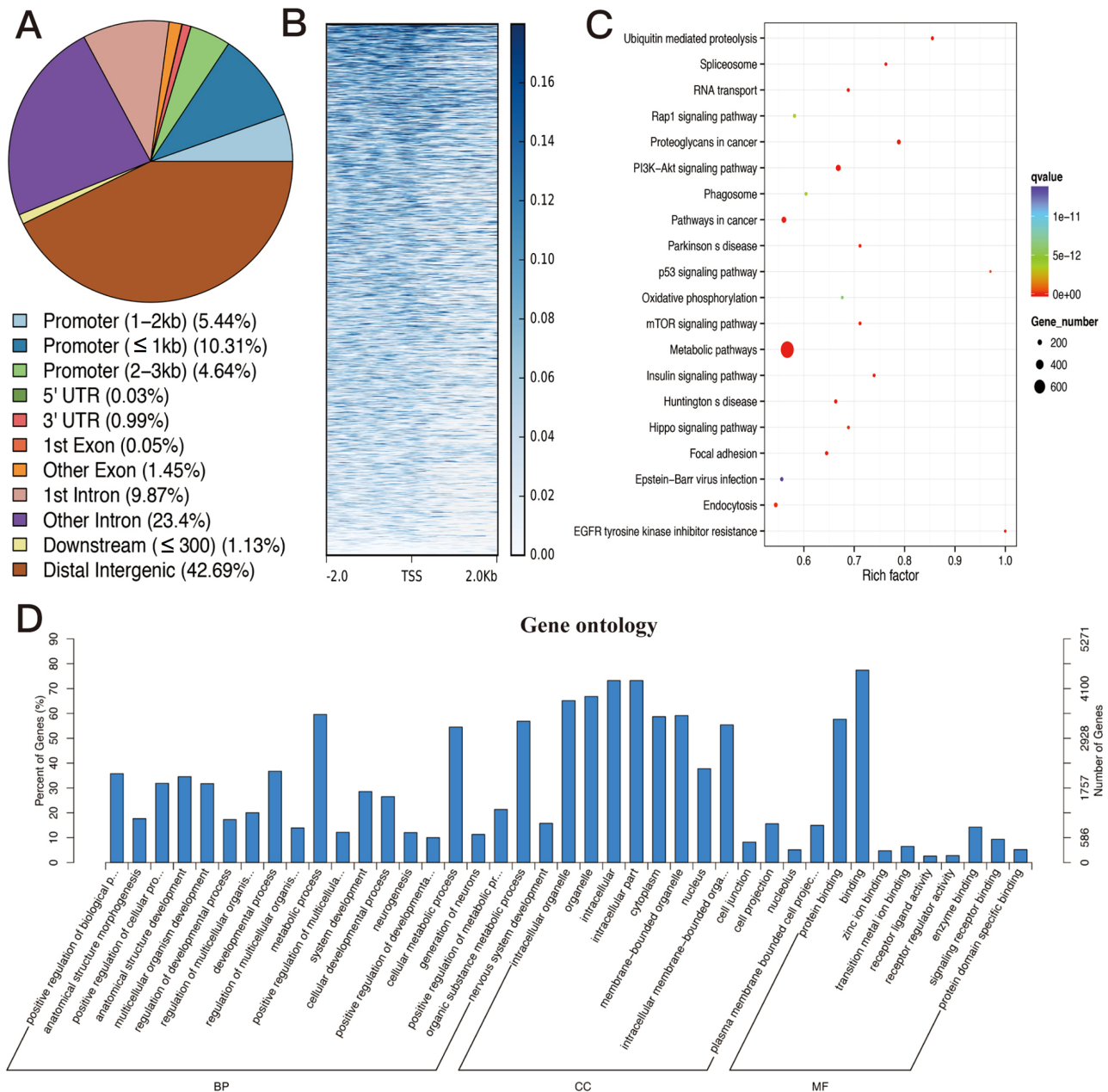


**Figure 7. Bioinformatics analysis following ChIP-seq targeting nuclear PAC1-R** (A) The nuclear PAC1-R binding regions mapped by ChIPseeker. (B) The distribution of the reads relative to gene TSS sites analyzed using computeMatrix of deepTools software. (C) KEGG pathway enrichment analysis of targets gene associated with peaks using KOBAS tool. The q-value is the corrected p-value and the range of q-value is (0,1). The lower the q-value, the more significant the enrichment. (D) Gene ontology (GO) enrichment analysis of PAC1-R using GOseq R package software. The top 41 terms were performed including BP (biological processes), CC (cellular components) and MF (molecular functions).

membrane or translocated into the nucleus can directly bind with nuclear transcription factors, DNA, etc., thereby efficiently regulating the body's biological processes, such as nuclear DNA synthesis, transcription, expression, and even protein modification. For instance, coagulation Factor II Receptor-like 1 (F2r1) on the cell membrane of RGC-5 cells promotes Angiogenin gene 1 through conventional signal transduction pathways, but cannot activate vascular endothelial growth factor A, while F2r1 in the nucleus can recruit transcription factor-specific protein 1 (SP1) by its C-terminal to promote the up-regulation of vascular endothelial growth factor-A expression[35,36]. In this research, the results of KEGG and GO

analysis following the ChIP-seq targeting the nuclear PAC1-R confirmed that many target genes of the nuclear PAC1-R are involved in pathways related to cellular stress, cell protection and neurodegenerative diseases (PD and Huntington's disease), and biological processes associated with the development and production of neurons. However, the working mechanisms of nuclear-translocated PAC1-R deserve deeper exploration.

Since the positive ChIP-PCR results confirmed that the nuclear PAC1-R can bind with the promoter sequence of *PACAP* and *PAC1-R*, and the dual-luciferases reporter assay confirmed that the nuclear PAC1-R up-regulates the promoter activities of *PACAP* and *PAC1-R*

in some way, we hypothesize that some transcription factors may be involved in the binding of nuclear PAC1-R with *PAC1-R* and *PACAP* promoters, especially the transcription factors shared by both *PAC1-R* and *PACAP* promoters. The results of transcription factor analysis indicated that 3 of the 6 common transcription factors are shared by both *PACAP* and *PAC1-R*, including *Zic2*, *REST* and *YY1*. *Zic2* has been reported to be involved in the regulation of *PACAP* and *PAC1-R* expression [30,31]. Therefore, in addition to *Zic2*, *REST* and *YY1* are also worthy of further study.

RE-1-silencing transcription factor (*REST*), also known as neuron-restrictive silencer factor (*NRSF*), represses gene expression by interacting with the neural-restrictive silencer element (*NRSE*)/repressor element 1 (*RE-1*) and then recruiting other factors including *mSin3* and *CoREST* by two repressor domains which are located at the N- and C-termini of *REST* [37]. The reported genes containing *RE-1* include *P2RY4*, *NPTXR*, *NRXN3*, *NTRK3*, *SYN1*, *NEFH*, *SYNPHY*, *GRIN2a*, *BDNF*, *L1CAM*, etc. [38], and most of them are related to neuronal functions, indicating that the *NRSE-NRSF* system mainly regulates genes related to neuronal functions. As an important neuropeptide, *PACAP* also has three silencing elements including *NRSLE1*, *NRSLE2*, and *NRSLE3*, which are highly homologous to *NRSE* and have a similar *REST* binding mode [39], indicating that the expression of *PACAP* is also controlled by the *NRSE-NRSF* system. Therefore, the nuclear *PAC1-R* may interfere with the silence effect of the *NRSE-NRSF* system on *PACAP* expression.

Furthermore, we hypothesize that the function of the *NRSE-NRSF* system may be regulated by nuclear *PAC1-R* in two ways: (1) directly by the binding with the C-terminus of the nuclear *PAC1-R*; and (2) indirectly by some key factors involved in the function of the *NRSE-NRSF* system, whose expression are regulated by nuclear

*PAC1-R*. For example, also as a neuroprotective protein, huntingtin (*Htt*) can interact with *REST* to maintain it in the cytoplasm and decrease the concentration of *REST* in the nuclear fraction, which can reduce the level of neutral gene silencing and finally allow the expression of genes containing *NRSE* element [40]. The expression of *Htt* has been reported to be mediated by *SP1*, which has been enriched and detected by ChIP-seq targeting nuclear *PAC1-R* [41]. So the nuclear-translocated *PAC1-R* may regulate the function of the *NRSE-NRSF* system indirectly by up-regulating the expression of *Htt*.

Based on the above analysis, we propose a working mechanism of the effect of nuclear translocation of *PAC1-R* on the expressions of *PAC1-R* and *PACAP*, which involves a positive allosteric regulation of *PAC1-R* (Figure 8). After the N-terminal extracellular domain of *PAC1-R* senses the allosteric modulation stimulation and *PAC1-R* undergoes nuclear translocation under the assistance of some kind of transporter proteins including importin/transportin/sortin/ $\beta$ -arrestin depending on the C-terminal nuclear translocation sequence of *PAC1-R* in some kind of endosome [23], the C-terminal fragment of *PAC1-R* is cleaved and transported into the nucleus, then the nuclear *PAC1-R* regulates the expressions of *PAC1-R* and *PACAP* in two ways: (1) the direct way in which the C-terminus of nuclear *PAC1-R* recruits transcription factors such as *SP1*, *Zic2*, *GATA1*, *REST* and *YY1*, or directly binds with the *PAC1-R/PACAP* promoter regions to enhance the promoter activities of *PAC1-R/PACAP* (Figure 8A); (2) the indirect way in which the C-terminus of nuclear *PAC1-R* recruits transcription factors to regulate the expressions of some key proteins such as *Htt*, and reduces the silencing activity related to *PACAP* by regulating the function of the *NRSE-NRSF* system (Figure 8B).

In summary, our findings demonstrate that the nuclear translo-

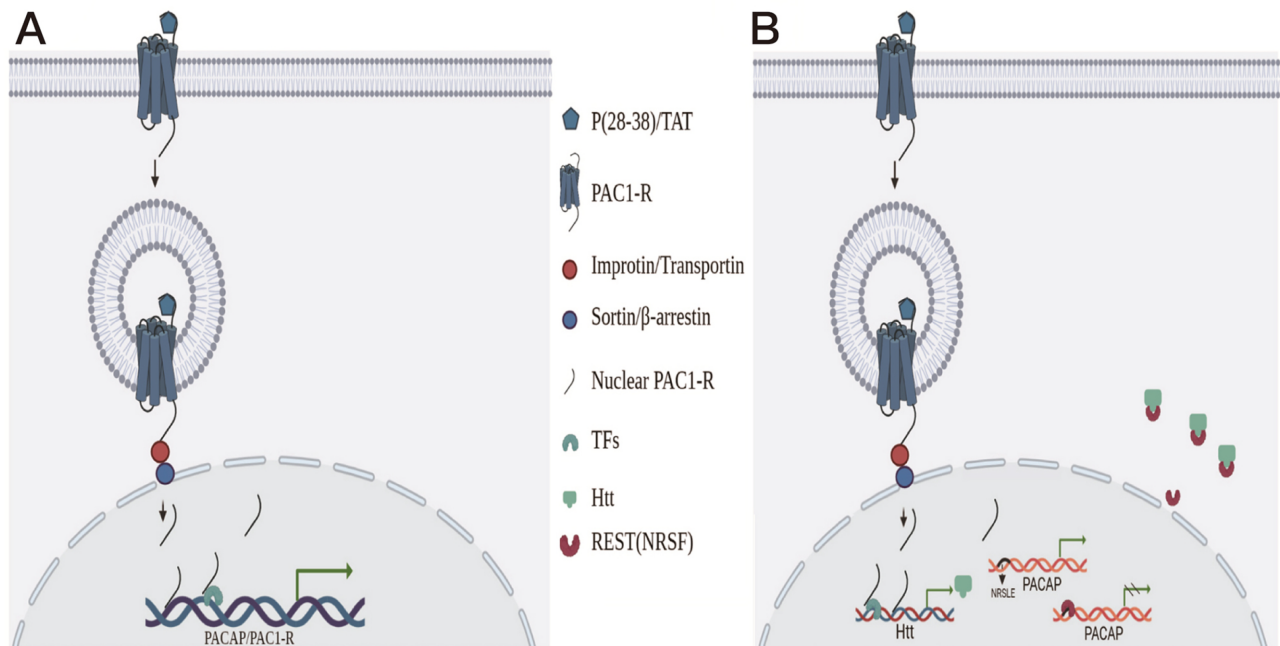


**Figure 8. The working mechanism of PAC1-R nuclear translocation and the signalling pathway mediated by nuclear PAC1-R** The binding of the allosteric modulators at the N-terminal extracellular domain of PAC1-R such as PACAP(28-38) and TAT trigger the significant endocytosis and nuclear translocation of PAC1-R; then the nuclear PAC1-R promotes the transcriptions of itself and its specific ligand PACAP in two ways. (A) The C-terminus of nuclear PAC1-R recruits TFs such as *SP1*, *Zic2*, *GATA1*, *REST*, *YY1*, or directly binding *PAC1-R/PACAP* promoter regions to enhance the promoters activities of *PAC1-R/PACAP*. (B) The C-terminus of nuclear PAC1-R recruits TFs to regulate some key protein expression such as *Htt* and reduces the silencer activity related to *PACAP* by regulating the function of *NRSE-NRSF* system.

cation of PAC1-R induced by the allosteric regulation of PAC1-R contributes to the up-regulation of the expression of itself and its specific ligand PACAP, and the nuclear PAC1-R works efficiently not only to enhance the promoter activities of *PAC1-R/PACAP*, but also to regulate a series of downstream target genes related to cell metabolism, cell stress, neuron protection, neuron development and neuron regeneration. Furthermore, we also reveal that the allosteric modulation site in the N-terminal extracellular domain of PAC1-R may work as a 'sensor' to sense the metabolite of PACAP38 such as PACAP(28-38) to keep the activity balance of the conserved PACAP/PAC1-R system or monitor the metabolite of oxidative stress such as some kind of ROS or some positively charged products like TAT to protect neurons with expression of PAC1-R against oxidative damage, or to help neurons make effective response to the oxidative stress.

### Acknowledgement

We thank Prof. Jian Zhang of Shanghai Jiao Tong University School of Medicine for providing the virtual screening and molecular docking service.

### Funding

This work was supported by the grants from the National Natural Science Foundation of China (Nos. 31100545 and 31670848) and the Natural Science Foundation of Guangdong Province (Nos. 2016A030313087 and 2022A1515011158).

### Conflict of Interest

The authors declare that they have no conflict of interest.

### References

- Pisegna JR, Oh DS. Pituitary adenylate cyclase-activating polypeptide: a novel peptide with protean implications. *Curr Opin Endocrinol Diabetes Obesit* 2007, 14: 58–62
- Harmar AJ, Arimura A, Gozes I, Journot L, Laburthe M, Pisegna JR, Rawlings SR, *et al.* International Union of Pharmacology. XVIII. Nomenclature of receptors for vasoactive intestinal peptide and pituitary adenylate cyclase-activating polypeptide. *Pharmacol Rev* 1998, 50: 265–270
- Lee EH, Seo SR. Neuroprotective roles of pituitary adenylate cyclase-activating polypeptide in neurodegenerative diseases. *BMB Rep* 2014, 47: 369–375
- Reglodi D, Atlasz T, Szabo E, Jungling A, Tamas A, Juhasz T, Fulop BD, *et al.* PACAP deficiency as a model of aging. *GeroScience* 2018, 40: 437–452
- Kasica N, Podlasz P, Sundvik M, Tamas A, Reglodi D, Kaleczyc J. Protective effects of pituitary adenylate cyclase-activating polypeptide (PACAP) against oxidative stress in zebrafish hair cells. *Neurotox Res* 2016, 30: 633–647
- Miyata A, Jiang L, Dahl RD, Kitada C, Kubo K, Fujino M, Minamino N, *et al.* Isolation of a neuropeptide corresponding to the N-terminal 27 residues of the pituitary adenylate cyclase activating polypeptide with 38 residues (PACAP38). *Biochem Biophys Res Commun* 1990, 170: 643–648
- Martínez C, Arranz A, Juarranz Y, Abad C, García-Gómez M, Rosignoli F, Leceta J, *et al.* PAC1 receptor: emerging target for septic shock therapy. *Ann NY Acad Sci* 2006, 1070: 405–410
- Seaborn T, Masmoudi-Kouli O, Fournier A, Vaudry H, Vaudry D. Protective effects of pituitary adenylate cyclase-activating polypeptide (PACAP) against apoptosis. *Curr Pharmaceutical Des* 2011, 17: 204–214
- Nakajima E, Walkup RD, Fujii A, Shearer TR, AzuMa M. Pituitary adenylate cyclase-activating peptide induces neurite outgrowth in cultured monkey trigeminal ganglion cells: involvement of receptor PAC1. *Mol Vis* 2013, 19: 174–83
- Solés-Tarrés I, Cabezas-Llobet N, Vaudry D, Xifró X. Protective effects of pituitary adenylate cyclase-activating polypeptide and vasoactive intestinal peptide against cognitive decline in neurodegenerative diseases. *Front Cell Neurosci* 2020, 14: 221
- Liao C, de Molliens MP, Schneebeil ST, Brewer M, Song G, Chatenet D, Braas KM, *et al.* Targeting the PAC1 receptor for neurological and metabolic disorders. *Curr Top Med Chem* 2019, 19: 1399–1417
- Shintani Y, Hayata-Takano A, Moriguchi K, Nakazawa T, Ago Y, Kasai A, Seiriki K, *et al.*  $\beta$ -Arrestin1 and 2 differentially regulate PACAP-induced PAC1 receptor signaling and trafficking. *PLoS ONE* 2018, 13: e0196946
- Dautzenberg FM, Mevenkamp G, Wille S, Hauger RL. N-terminal splice variants of the type I PACAP receptor: isolation, characterization and ligand binding/selectivity determinants. *J Neuroendocrinol* 1999, 11: 941–949
- Gourlet P, Woussen-Colle MC, Robberecht P, de Neef P, Cauvin A, Vandermeers-Piret MC, Vandermeers A, *et al.* Structural requirements for the binding of the pituitary adenylate-cyclase-activating peptide to receptors and adenylate-cyclase activation in pancreatic and neuronal membranes. *Eur J Biochem* 1991, 195: 535–541
- Robberecht P, Gourlet P, De Neef P, Woussen-Colle MC, Vandermeers-Piret MC, Vandermeers A, Christophe J. Structural requirements for the occupancy of pituitary adenylate-cyclase-activating-peptide (PACAP) receptors and adenylate cyclase activation in human neuroblastoma NB-OK-1 cell membranes. Discovery of PACAP(6-38) as a potent antagonist. *Eur J Biochem* 1992, 207: 239–246
- Yu R, Zheng L, Cui Y, Zhang H, Ye H. Doxycycline exerted neuroprotective activity by enhancing the activation of neuropeptide GPCR PAC1. *Neuropharmacology* 2016, 103: 1–15
- Song S, Wang L, Li J, Huang X, Yu R. The allosteric modulation effects of doxycycline, minocycline, and their derivatives on the neuropeptide receptor PAC1-R. *Acta Biochim Biophys Sin* 2019, 51: 627–637
- Yu R, Yang Y, Cui Z, Zheng L, Zeng Z, Zhang H. Novel peptide VIP-TAT with higher affinity for PAC1 inhibited scopolamine induced amnesia. *Peptides* 2014, 60: 41–50
- Yu R, Li J, Lin Z, Ouyang Z, Huang X, Reglodi D, Vaudry D. TAT-tagging of VIP exerts positive allosteric modulation of the PAC1 receptor and enhances VIP neuroprotective effect in the MPTP mouse model of Parkinson's disease. *Biochim Biophys Acta* 2020, 1864: 129626
- Zhu L, Tamvakopoulos C, Xie D, Dragovic J, Shen X, Fenyk-Melody JE, Schmidt K, *et al.* The role of dipeptidyl peptidase IV in the cleavage of glucagon family peptides. *J Biol Chem* 2003, 278: 22418–22423
- Meloni BP, Brookes LM, Clark VW, Cross JL, Edwards AB, Anderton RS, Hopkins RM, *et al.* Poly-arginine and arginine-rich peptides are neuroprotective in stroke models. *J Cereb Blood Flow Metab* 2015, 35: 993–1004
- Yu R, Zhong J, Li M, Guo X, Zhang H, Chen J. PACAP induces the dimerization of PAC1 on the nucleus associated with the cAMP increase in the nucleus. *Neurosci Lett* 2013, 549: 92–96
- Yu R, Lin Z, Ouyang Z, Tao Z, Fan G. Blue light induces the nuclear translocation of neuropeptide receptor PAC1-R associated with the up-regulation of PAC1-R its own in reactive oxygen species associated way. *Biochim Biophys Acta* 2021, 1865: 129884
- Yu R, Guo X, Zhong J, Li M, Zeng Z, Zhang H. The N-terminal HSDC1F motif is required for cell surface trafficking and dimerization of family B G protein coupled receptor PAC1. *PLoS ONE* 2012, 7: e51811
- Yu R, Cui Z, Li M, Yang Y, Zhong J. Dimer-dependent intrinsic/basal activity of the class B G protein-coupled receptor PAC1 promotes cellular

- anti-apoptotic activity through wnt/ $\beta$ -catenin pathways that are associated with dimer endocytosis. *PLoS ONE* 2014, 9: e113913
26. Messegueur X, Escudero R, Farré D, Núñez O, Martínez J, Albà MM. PROMO: detection of known transcription regulatory elements using species-tailored searches. *Bioinformatics* 2002, 18: 333–334
  27. Zhang Q, Liu W, Zhang HM, Xie GY, Miao YR, Xia M, Guo AY. hTFtarget: a comprehensive database for regulations of human transcription factors and their targets. *Genomics Proteomics Biolnf* 2020, 18: 120–128
  28. Safran M, Dalah I, Alexander J, Rosen N, Iny Stein T, Shmoish M, Nativ N, *et al.* GeneCards Version 3: the human gene integrator. *Database* 2010, 2010: baq020
  29. Fornes O, Castro-Mondragon JA, Khan A, van der Lee R, Zhang X, Richmond PA, Modi BP, *et al.* JASPAR 2020: update of the open-access database of transcription factor binding profiles. *Nucleic Acids Res* 2019, 48: D87
  30. Hoffmann A, Ciani E, Houssami S, Brabet P, Journot L, Spengler D. Induction of type I PACAP receptor expression by the new zinc finger protein Zac1 and p53. *Ann NY Acad Sci* 1998, 865: 49–58
  31. Ciani E, Hoffmann A, Schmidt P, Journot L, Spengler D. Induction of the PAC1-R (PACAP-type I receptor) gene by p53 and Zac. *Mol Brain Res* 1999, 69: 290–294
  32. Thomas RL, Crawford NM, Grafer CM, Zheng W, Halvorson LM. GATA augments GnRH-mediated increases in *Adcyap1* gene expression in pituitary gonadotrope cells. *J Mol Endocrinol* 2013, 51: 313–324
  33. Miura A, Kambe Y, Inoue K, Tatsukawa H, Kurihara T, Griffin M, Kojima S, *et al.* Pituitary adenylate cyclase-activating polypeptide type 1 receptor (PAC1) gene is suppressed by transglutaminase 2 activation. *J Biol Chem* 2013, 288: 32720–32730
  34. Bhosle VK, Rivera JC, Chemtob S. New insights into mechanisms of nuclear translocation of G-protein coupled receptors. *Small GTPases* 2017, 10: 1–10
  35. Joyal JS, Nim S, Zhu T, Sitaras N, Rivera JC, Shao Z, Sapieha P, *et al.* Subcellular localization of coagulation factor II receptor-like 1 in neurons governs angiogenesis. *Nat Med* 2014, 20: 1165–1173
  36. Joyal JS, Bhosle VK, Chemtob S. Subcellular G-protein coupled receptor signaling hints at greater therapeutic selectivity. *Expert Opin Therapeutic Targets* 2015, 19: 717–721
  37. Lee LTO, Lee VHY, Yuan PY, Chow BKC. Identification of repressor element 1 in secretin/PACAP/VIP genes. *Ann NY Acad Sci* 2006, 1070: 388–392
  38. Bruce AW, Donaldson IJ, Wood IC, Yerbury SA, Sadowski MI, Chapman M, Göttgens B, *et al.* Genome-wide analysis of repressor element 1 silencing transcription factor/neuron-restrictive silencing factor (REST/NRSF) target genes. *Proc Natl Acad Sci USA* 2004, 101: 10458–10463
  39. Sugawara H, Tominaga A, Inoue K, Takeda Y, Yamada K, Miyata A. Functional characterization of neural-restrictive silencer element in mouse pituitary adenylate cyclase-activating polypeptide (PACAP) gene expression. *J Mol Neurosci* 2014, 54: 526–534
  40. Zuccato C, Tartari M, Crotti A, Goffredo D, Valenza M, Conti L, Cataudella T, *et al.* Huntingtin interacts with REST/NRSF to modulate the transcription of NRSE-controlled neuronal genes. *Nat Genet* 2003, 35: 76–83
  41. Qiu Z, Norflus F, Singh B, Swindell MK, Buzescu R, Bejarano M, Chopra R, *et al.* Sp1 is up-regulated in cellular and transgenic models of Huntington disease, and its reduction is neuroprotective. *J Biol Chem* 2006, 281: 16672–16680